6050 *Macromolecules* **2009**, *42*, 6050–6055
DOI: 10.1021/ma9010507

Macromolecules
ARTICLE

Temperature Effect on Activation Rate Constants in ATRP: New Mechanistic Insights into the Activation Process

Florian Seeliger and Krzysztof Matyjaszewski*

Center for Macromolecular Engineering, Department of Chemistry, Carnegie Mellon University, 4400 Fifth Avenue, Pittsburgh, Pennsylvania 15213

Received May 13, 2009; Revised Manuscript Received June 17, 2009

ABSTRACT: Activation rate constants (k_{act}) for a variety of initiators for Cu-mediated ATRP were measured with Cu(I)Br(PMDETA) at various temperatures (i.e., −40 to +60 °C). Reactions of less active alkyl halides were more accelerated by increased temperatures than reactions of more active initiators. Straight Eyring and Arrhenius plots were obtained, from which the activation parameters (i.e., $\Delta H^{\ddagger}$, $\Delta S^{\ddagger}$, E_a, and ln A) were determined. The activation enthalpies $\Delta H^{\ddagger}$ are in between 26.0 and 38.7 kJ mol^{-1} with highly negative activation entropies ($\Delta S^{\ddagger} = -156$ to -131 J mol^{-1} K^{-1}), which indicate greatly ordered structures of the transition states for these reactions.

Introduction

Atom transfer radical polymerization (ATRP) is a powerful and robust polymerization technique for the synthesis of polymeric materials with well-defined compositions, architectures, and functionalities.[1−8] The key concept of this technique is to provide fast initiation and minimize irreversible termination reactions by a reduced radical concentration during the polymerization.[8−11] This is achieved by a transition metal complex which finely adjusts the equilibrium between dormant polymer chains and active radicals (Scheme 1).[12,13]

In a reversible activation step, a halogen atom is abstracted from the dormant species (P_n−X) by a transition metal complex, yielding an active chain end and a transition metal complex in the higher oxidation state. This homolytic cleavage of the P_n−X bond proceeds with a rate constant k_{act}. The formed alkyl radical ($P_n^{\bullet}$) adds to the monomer with a propagation rate constant k_p, before it is deactivated with a rate constant k_{deact} by the metal complex in its higher oxidation state (XMt^{z+1}L$_m$Y). The contribution of termination becomes insignificant due to the persistent radical effect,[14−16] and therefore, polymers are formed with low polydispersities and molecular weights that linearly increase with conversion.[17,18]

From eqs 1 and 2 one can directly see that k_{act} and k_{deact}, which determine the ATRP equilibrium ($K_{ATRP} = k_{act}/k_{deact}$), contribute to the rate of polymerization (R_p) and the evolution of polydispersity (M_w/M_n).[19] Therefore, all factors which influence these rate constants are critically important for understanding the controlled polymerization process and are inherently part of the foundation for future developments in ATRP.

$$R_p = k_p[M]\frac{k_{act}[P_n{-}X]_0[Mt^z L_m Y]_0}{k_{deact}[X{-}Mt^{z+1}L_m Y]_0} \quad (1)$$

$$\frac{M_w}{M_n} = 1+\left(\frac{k_p[I]_0}{k_{deact}[X{-}Mt^{z+1}L_m Y]}\right)\left(\frac{2}{p}-1\right) \quad (2)$$

Several activation rate constants (k_{act}) for initiator/catalyst combinations have been previously measured.[8,9,13,20−37] The effects of initiator,[30,31,37] monomer,[31] counterion,[27,30,31] ligand,[13,24,31,35] [ligand]/[Cu(I)] ratio,[30,31,35] solvent,[23,30,31,35] Cu(II) concentration,[34] and the penultimate unit[32] on the activation kinetics in ATRP have been thoroughly studied. However, the employed chromatographic methods are not accurate enough to precisely study the effect of temperature (i.e., the determination of activation parameters) on the activation step. This is due to the fact that these indirect techniques usually require sampling and filtration through alumina of the reaction mixture after certain time intervals. In the case of analysis by gas chromatography with electron capture detector and trichlorobenzene as internal standard, the error of kinetic experiments was within 30%.[37] This relatively large error in these experiments is also caused by the inevitable need of excess of Cu(I) complex over the alkyl halide. Any remaining or introduced oxygen in the reaction flask reduces the apparent Cu(I) concentration by fast oxidation to the corresponding Cu(II) complex and thus falsifies the result.

In 2004, stopped-flow equipment was used to directly follow the concentration of the accumulating persistent radical (i.e., the Cu(II) species) in reactions of highly reactive alkyl halides with highly reactive (i.e., strongly reducing) copper(I) complexes.[33] This UV−vis method allows a much more accurate determination of the activation rate constant (k_{act}). Therefore, this analytical method is preferred over chromatographic techniques. Herein, we report detailed UV−vis spectroscopic studies on the effect of temperature and initiator structure on the activation process in ATRP using an immersion probe equipped with fiber optics. The obtained temperature-dependent rate constants (k_{act}) were accurate enough to determine activation parameters of these reactions, which provide us with a more detailed understanding of the ATRP mechanism. However, one has to keep in mind that the activation process is only one part of the ATRP equilibrium. Studies of temperature effect on K_{ATRP} are currently underway.

Experimental Section

Materials. Bromoacetonitrile (BrAN, 97%, Aldrich), 2-bromopropionitrile (BrPN, 97%, Aldrich), methyl 2-bromoisobutyrate (MBriB, 99%, Aldrich), ethyl 2-bromoisobutyrate (EtBriB, 99%, Aldrich), methyl 2-bromopropionate (MBrP, 98%, Aldrich), 2-chloropropionitrile (ClPN, 95%, Aldrich),

*Corresponding author. E-mail: km3b@andrew.cmu.edu.

 Published on Web 07/10/2009

Scheme 1. Proposed Mechanism for ATRP

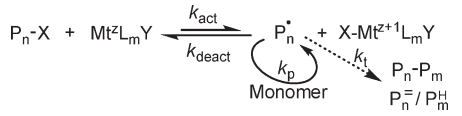

Scheme 2. Structures of Studied Alkyl Halides

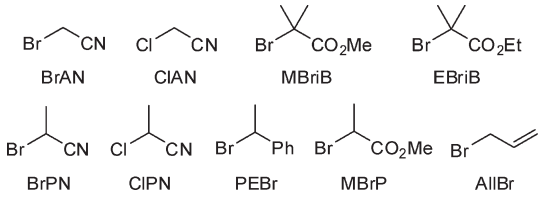

Scheme 3. Isolation of the Activation Process by Irreversible Trapping of the Formed Radicals with TEMPO

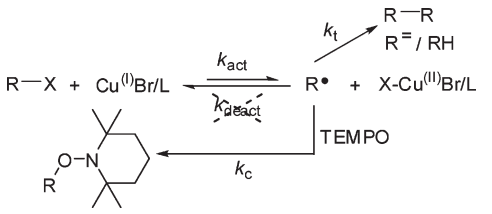

chloroacetonitrile (ClAN, 99%, Aldrich), allyl bromide (AllBr, 97%, Aldrich), 1-(bromoethyl)benzene (PEBr, 97%, Aldrich), and *N,N,N′,N′,N″*-pentamethyldiethylenetriamine (PMDETA, 99%, Aldrich) were distilled prior to use. Copper(I) bromide (99.999%, Aldrich), 2,2,6,6-tetramethylpiperidinyl-1-oxy (TEMPO, 99%, Aldrich), and acetonitrile (MeCN, HPLC-grade, Fisher) were used as received. All other reagents were used as received.

Typical Procedure for the Measurement of Activation Rate Constants (Cu(I)Br/PMDETA with Methyl 2-Bromopropionate (MBrP)). Stock solutions of Cu(I)Br (5×10^{-2} mol L^{-1}), PMDETA (2×10^{-1} mol L^{-1}), TEMPO (6×10^{-1} mol L^{-1}), and methyl 2-bromopropionate (MBrP, 1 mol L^{-1}) in MeCN were prepared in 5 mL volumetric flasks sealed with rubber septa. These solutions were degassed in an ultrasonic bath (10 min) and subsequently purged with N_2 (15 min). Calculated amounts of Cu(I)Br, PMDETA, TEMPO, and additional degassed MeCN were then transferred via N_2-purged, gastight syringes into an oxygen-free Schlenk flask, which was equipped with a Hellma UV−vis immersion probe and a stir bar. The reaction was then started by the addition of alkyl halide to the stirred solution. During all kinetic studies the temperature of the solutions was controlled (±0.1 °C) by using a Haake K50 circulating bath thermostat. For the evaluation of kinetics a Varian Cary 5000 UV−vis−NIR spectrophotometer was used.

Method. The activation rate constants were determined by UV−vis spectroscopy using trapping experiments with TEMPO. The radicals originating from homolytic halogen abstraction from the alkyl halides are irreversibly trapped by this stable nitroxide radical to yield the corresponding alkoxyamines (Scheme 3).[26,38] This process is so fast[39] (i.e., close to the diffusion limit) that the use of 10 equiv of TEMPO with respect to the Cu(I) complex guarantees immediate trapping with no transformation back to the dormant species. A separate experiment proved that TEMPO is not capable of oxidizing Cu(I)Br(PMDETA) to the corresponding Cu(II) complex under these conditions (see Supporting Information, p 1). The kinetic experiments were performed under pseudo-first-order conditions[40] using a large excess of alkyl halide. The reactions were monitored by following the increase of the UV−vis absorbance at 740 nm which corresponds to the λ_{max} of the formed Cu(II) complexes.

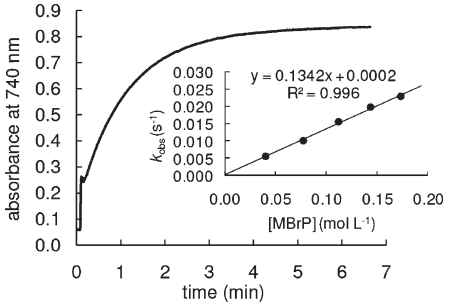

Figure 1. Exponential increase of the absorbance at 740 nm during the reaction of Cu(I)Br/PMDETA ($c_0 = 3.71 \times 10^{-3}$ mol L^{-1}) with methyl 2-bromopropionate (MBrP, $c_0 = 1.11 \times 10^{-1}$ mol L^{-1}) in MeCN at 20 °C. Inset: plot of k_{obs} vs [MBrP] to yield the second-order activation rate constant (k_{act}).

From the exponential increases of the UV−vis absorbances the pseudo-first-order rate constants were obtained by fitting the single exponential $y = A[1 - \exp(-k_{obs}t)] + C$ to the observed time-dependent Cu(II) absorbance (Figure 1). The second-order rate constants (k_{act}) (Table 1) are then obtained as the slopes of k_{obs} vs [alkyl halide] correlations (Figure 1, inset).

Results

In order to verify the utilized pseudo-first-order kinetic method, we also studied second-order kinetics in one case. The reaction of exact equimolar amounts of ethyl 2-bromoisobutyrate (EtBriB) and Cu(I)Br(PMDETA) was followed at 0 °C in MeCN. With the previously determined extinction coefficient (740 nm) of Cu(II)Br_2(PMDETA), the obtained absorbance−time run was transformed into time-dependent absolute concentrations of the Cu(II) complex. A plot of $1/[Cu(I)Br(PMDETA)]_0 - [Cu(II)Br_2(PMDETA)]$ vs time yielded a straight line from which the second-order rate constant $k_{act} = 8.83 \times 10^{-1}$ L mol^{-1} s^{-1} was determined (Figure 2).

The same reaction was then studied at 0 °C using the described pseudo-first-order technique (i.e., 10-fold excess of the initiator over the Cu catalyst). The obtained activation rate constant ($k_{act} = 9.48 \times 10^{-1}$ L mol^{-1} s^{-1}, Table 1) is only 7.4% larger, which indicates good reproducibility and validates the pseudo-first-order kinetic method.

The temperature effect on the activation rate constant was studied with three α-bromoesters, four α-halonitriles, two benzyl bromides, and allyl bromide as initiators (Scheme 3) and Cu(I)Br(PMDETA) as catalyst. The reactions of the most active tertiary α-bromoesters methyl and ethyl 2-bromoisobutyrate (MBriB, EtBriB), as well as bromoacetonitrile (BrAN) were studied in a temperature range from −40 to +40 °C. At higher temperatures (e.g., 60 °C) the reactions of these initiators were too fast to be precisely measured. 2-Bromopropionitrile (BrPN) is already so active that kinetics could only be measured at temperatures below −15 °C. All other alkyl halides were studied in a temperature range from −20 to +60 °C due to sufficiently slow reactions with Cu(I)Br(PMDETA) at temperatures below −20 °C.

Discussion

On the basis of the temperature dependence of the activation rate constants (k_{act}), the magnitudes of the activation enthalpy ($\Delta H^{\ddagger}$) and activation entropy ($\Delta S^{\ddagger}$) as well as activation energy (E_a) were determined (Table 2) by evaluation of the resulting straight Eyring correlations (Figure 3).[41] The error levels were calculated from the standard deviation of the Eyring and

Table 1. Second-Order Rate Constants k_{act} (L mol^{-1} s^{-1}, MeCN) of the Reactions of Cu(I)Br(PMDETA) with Alkyl Halides at Different Temperatures

[a]	−40 °C	−20 °C	0 °C	20 °C	40 °C	60 °C	
BrAN	1.40×10^{-1}	4.93×10^{-1}	1.56	3.91	7.88		
MBriB	1.21×10^{-1}	4.49×10^{-1}	1.21	2.38	4.68		
EtBriB	1.00×10^{-1}	3.47×10^{-1}	9.48×10^{-1}	1.75	4.08		
MBrP		1.60×10^{-2}	5.68×10^{-2}	1.34×10^{-1}	3.41×10^{-1}	7.27×10^{-1}	
ClPN		9.34×10^{-3}	3.84×10^{-2}	1.19×10^{-1}	2.43×10^{-1}	5.52×10^{-1}	
PEBr		9.87×10^{-3}	2.88×10^{-2}	9.73×10^{-2}	2.47×10^{-1}	6.08×10^{-1}	
ClAN		5.10×10^{-3}	1.71×10^{-2}	5.89×10^{-2}	1.36×10^{-1}	2.92×10^{-1}	
AllBr		2.84×10^{-3}	9.12×10^{-3}	3.80×10^{-2}	1.05×10^{-1}	2.97×10^{-1}	
	−41 °C	−39 °C	−36.5 °C	−32 °C	−28.5 °C	−23 °C	−15 °C
BrPN	1.05	1.14	1.38	1.81	2.05	2.80	4.64

[a] See Figure 1 for structures.

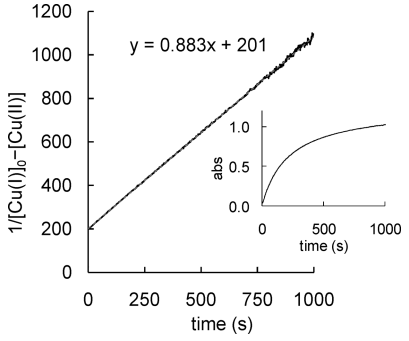

Figure 2. Second-order kinetics of the reaction of ethyl bromoisobutyrate (EtBriB, $c_0 = 5.09$ mM) with Cu(I)Br(PMDETA) ($c_0 = 5.08$ mM) at 0 °C in MeCN. Inset: corresponding absorbance−time run at 740 nm.

Arrhenius plots for the logarithmic values of the rate constants versus $1/T$.

Comparison of measured activation free energies ($\Delta G^{\ddagger}$) at 20 °C with calculated free energies for the homolytic cleavage of alkyl halides in MeCN at 20 °C (ΔG_{BDE})[42] indicates that the strength of the breaking R−X bond is a significant contributing factor in governing the barrier height of the activation process. As can be seen in Figure 4, a plot of $\Delta G^{\ddagger}$ vs ΔG_{BDE} yields a good correlation for the reactions of alkyl bromides with Cu(I)Br-(PMDETA). However, both α-chloronitriles (ClPN, ClAN) do not correlate. This is due to the fact that copper catalysts are more chloro- than bromophilic and, therefore, compensate high bond dissociation energies for C−Cl bonds.[12]

Initiator Structure. For a comparison of absolute reactivities of all studied initiators, the rate constants at 20 °C were evaluated. Because the reaction of 2-bromopropionitrile (BrPN) with Cu(I)Br(PMDETA) was too fast to be studied at temperatures higher than −15 °C, k_{act} at 20 °C was determined from the obtained Eyring parameters. With $\Delta H^{\ddagger} = 26.0$ kJ mol^{-1} and $\Delta S^{\ddagger} = -131$ J mol^{-1} K^{-1} (Table 2, first entry) one calculates $k_{act}(20\ °C) = 2.05 \times 10^{1}$ L mol^{-1} s^{-1} for the activation of BrPN by Cu(I)Br(PMDETA) (eq 3).

$$k_{act}(T) = \frac{k_b T}{h} e^{(-\Delta H - T\Delta S)/RT} \quad (3)$$

This value shows that BrPN is by far the most active initiator employed in this work followed by bromoacetonitrile (BrAN) and the two tertiary α-bromoesters (Figure 5), which is in agreement with previous studies on the effect of initiator on the activation rate constant.[37]

The secondary α-bromoester methyl 2-bromopropionate (MBrP) is ~1 order of magnitude less active than the tertiary α-bromoesters at 20 °C. The secondary initiators 2-chloropropionitrile (ClPN) and 1-bromo-1-phenylethane (PEBr) follow closely, and the investigated primary alkyl halides (chloroacetonitrile (ClAN), allyl bromide (AllBr), and benzyl bromide (BzBr)) are the least active substrates in this series. Therefore, the general reactivity order for alkyl halides in ATRP is tertiary > secondary > primary, which is in agreement with the resulting radical stability[43] and consistent with an inner-sphere electron-transfer process.[42]

The substituent in the alkyl ester group has a small effect on the reactivity as can be seen from the activation rate constants for tertiary methyl and ethyl bromoesters (e.g., MBriB and EtBriB). For different radical-stabilizing groups in the α-position, one generally finds the reactivity order nitrile > ester > benzyl, which is in accordance with calculated bond dissociation energies (BDE) by DFT methods.[42,44]

Temperature Effect. With the activation parameters at hand, one can easily determine activation rate constants at temperatures that are experimentally not accessible. For a comparison of the temperature effect on k_{act}, the activation rate constants at −40 °C for the least reactive alkyl halides (e.g., methyl 2-bromopropionate (MBrP), allyl bromide (AllBr)) and at +60 °C for the most active initiators (Figure 6) were calculated according to eq 3. One finds that the reaction with 2-bromopropionitrile (BrPN) is accelerated by a factor of 80 when increasing the temperature from −40 to +60 °C. The reactions of all other initiators are affected even more in this temperature range. The increased rates at 60 °C compared to the corresponding values at −40 °C for the halogen abstraction from methyl 2-bromoisobutyrate (MBriB, ×84), methyl 2-bromopropionate (MBrP, ×168), 1-bromo-1-phenylethane (PEBr, ×279), and allyl bromide (AllBr, ×587) indicate that less reactive initiators are more affected by this temperature jump. This effect can be anticipated because reactions with higher activation barriers ($\Delta G^{\ddagger}$) are normally more accelerated by increased temperatures than reactions with smaller values for the Gibbs free energy of activation (eq 4).

$$\frac{k_{act}(T_1)}{k_{act}(T_2)} = \frac{T_1}{T_2} e^{(\Delta G(T_2)/RT_2) - (\Delta G(T_1)/RT_1)} \quad (4)$$

Activation Parameter Analysis. All obtained activation entropies are highly negative, indicating that degrees of freedom (i.e., translational, rotational, and vibrational) are lost when approaching the transition state. Thus, the activation process is entropically disfavored which is common for bimolecular reactions.[45] Solvation can have a large impact on activation entropies, if a significant amount of ordering is required in the solvent to make favorable enthalpic interactions with the transition state.[41] However, for the comparison of the obtained activation entropies, such a solvent effect can be neglected because the solvent (MeCN) was not

Table 2. Activation Rate Constants, Activation Free Energy (20 °C), and Eyring and Arrhenius Parameters for the Reactions of Alkyl Halides with Cu(I)Br/PMDETA in MeCN

	k_{act}(20 °C) (L mol^{-1} s^{-1})	$\Delta G^{\ddagger}$(20 °C) (J mol^{-1} K^{-1})	$\Delta H^{\ddagger}$ (kJ mol^{-1})	$\Delta S^{\ddagger}$ (J mol^{-1} K^{-1})	E_a (kJ mol^{-1})	ln A
BrPN	2.05×10^{1} [a]	64.4	26.0 ± 0.9	−131 ± 4	28.1 ± 0.9	14.6 ± 0.4
BrAN	4.93×10^{-1}	68.6	28.7 ± 0.6	−136 ± 2	30.9 ± 0.6	14.0 ± 0.2
MBriB	4.49×10^{-1}	69.5	25.2 ± 0.9	−151 ± 3	27.5 ± 0.9	12.1 ± 0.4
EtBriB	3.47×10^{-1}	70.2	25.3 ± 0.8	−153 ± 3	27.5 ± 0.8	12.0 ± 0.3
MBrP	1.60×10^{-2}	76.5	30.8 ± 0.6	−156 ± 2	33.2 ± 0.6	11.7 ± 0.2
ClPN	9.34×10^{-3}	77.2	32.9 ± 1.4	−151 ± 5	35.3 ± 1.3	12.2 ± 0.6
PEBr	9.87×10^{-3}	77.4	34.0 ± 1.0	−148 ± 3	36.4 ± 1.0	12.6 ± 0.4
ClAN	5.10×10^{-3}	78.8	33.4 ± 0.8	−155 ± 3	35.8 ± 0.8	11.7 ± 0.3
AllBr	2.84×10^{-3}	79.7	38.7 ± 1.3	−140 ± 4	41.1 ± 1.3	13.6 ± 0.5

[a] Value was calculated from Eyring parameters and eq 3.

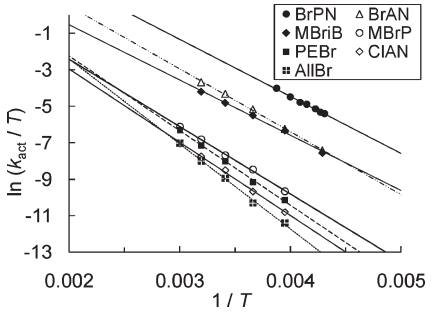

Figure 3. Eyring plots for the reactions of alkyl halides with Cu(I)Br-(PMDETA) in MeCN. For reasons of figure clarity the correlations for ethyl 2-bromoisobutyrate (EtBriB) and 2-chloropropionitrile (ClPN) were not depicted.

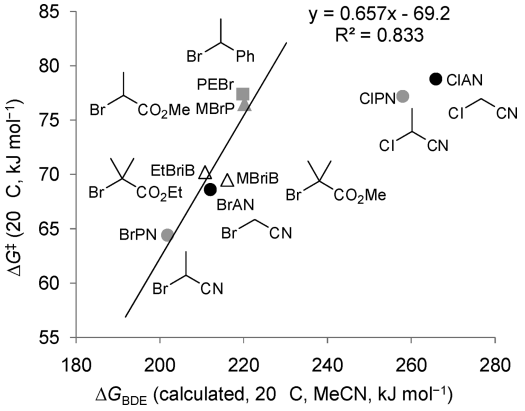

Figure 4. Plot of activation free energy ($\Delta G^{\ddagger}$, 20 °C, Table 2) vs calculated free energies (ΔG_{BDE}) of the homolytic cleavage of alkyl halides (R−X → R$^{\bullet}$ + X$^{\bullet}$, MeCN, 20 °C).[42] Black symbols: primary; gray: secondary; open: tertiary alkyl halides; circle: nitrile; square: benzyl; triangle: ester.

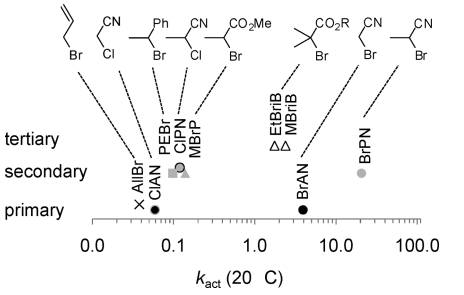

Figure 5. ATRP activation rate constants k_{act} (L mol^{-1} s^{-1}) for various initiators (black symbols: primary; gray: secondary; open: tertiary alkyl halides; circle: nitrile; square: benzyl; triangle: ester) with Cu(I)Br-(PMDETA) in MeCN at 20 °C. The value for 2-bromopropionitrile (BrPN) was calculated with Eyring parameters and eq 3.

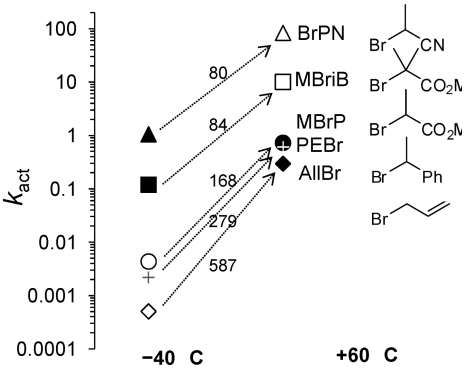

Figure 6. Effect of increased temperature (−40 to +60 °C) on activation rate constants (k_{act}) for selected alkyl halides with Cu(I)Br-(PMDETA). Filled symbols: experimental data; open symbols: calculated values from Eyring parameters and eq 3.

changed during this series. In addition, conformational changes of the Cu(PMDETA) catalyst are considered similar for the reactions with different alkyl halides.

With $\Delta S^{\ddagger} = -131$ J mol^{-1} K^{-1} (BrPN) and $\Delta S^{\ddagger} = -136$ J mol^{-1} K^{-1} (BrAN), the reactions of α-bromonitriles show the largest (i.e., the least negative) activation entropies of all studied alkyl bromides. This may be due to the sterically less demanding nitrile moiety, which allows a greater flexibility of the activated complex. As illustrated in Figure 3, the reaction of the small allyl bromide (AllBr) shows a comparably high value for $\Delta S^{\ddagger}$ (−140 J mol^{-1} K^{-1}). On the other hand, the discussion of activation entropies cannot solely be based on steric effects, as the reaction with the secondary 2-bromopropionitrile (BrPN) has larger activation entropy than the primary bromoacetonitrile (BrAN). This trend is also found for the couple 2-chloropropionitrile (ClPN, −151 J mol^{-1} K^{-1}) versus chloroacetonitrile (ClAN, −155 J mol^{-1} K^{-1}) and for the tertiary methyl 2-bromoisobutyrate (MBriB, −151 J mol^{-1} K^{-1}) versus the secondary methyl 2-bromopropionate (MBrP, −156 J mol^{-1} K^{-1}). Thus, a higher degree of methylation yields larger activation entropies, which corresponds to less rigid structures at the transition state.

According to Hammond's postulate,[46] the structure of the transition state resembles the structures of the products for endothermic reactions. For the ATRP activation process this means that the formation of the new copper−halogen bond is already well established at the transition state. Moreover, the more endothermic this reaction, the shorter is the Cu−halogen distance in the transition state.[47] It is well-known that homolytic cleavage of the carbon−halogen bond is most endothermic for primary alkyl halides followed by secondary

and tertiary ones. Therefore, a lower degree of substitution in α-position should result in shorter Cu−halogen distances at the transition state. Primary initiators have to come closer to the metal center than secondary initiators at the expense of losing degrees of freedom. In accordance, one finds that larger activation entropies for "more" methylated compounds always go along with smaller activation enthalpies (Table 2), which reflect the order of corresponding reaction enthalpies (Bell−Evans−Polanyi principle).[48] For the same reason, the activation entropies for the reactions of α-chloronitriles (ClPN, −151 J mol^{-1} K^{-1}; ClAN, −155 J mol^{-1} K^{-1}) are more negative than those of the corresponding bromo derivatives: shorter C−Cl and Cu(II)−Cl bonds compared to the corresponding C−Br and Cu(II)−Br bonds require a more congested and entropically less favored transition state.

Looking at steric effects not associated with the reaction center, one finds that the reaction with ethyl 2-bromoisobutyrate (EtBriB, $\Delta S^{\ddagger} = -153$ J mol^{-1} K^{-1}) is as expected more entropically controlled than the reaction with methyl 2-bromoisobutyrate (MBriB, $\Delta S^{\ddagger} = -151$ J mol^{-1} K^{-1}).

The comparison of bromoacetonitrile (BrAN) and MBriB, two initiators with different radical-stabilizing groups and similar reactivity at 20 °C (Figure 5), nicely illustrates the interplay between activation enthalpy and activation entropy (Figure 3). For enthalpy-controlled reactions (i.e., low temperature), MBriB ($\Delta H^{\ddagger} = 25.2$ kJ mol^{-1}) is more active than BrAN ($\Delta H^{\ddagger} = 28.7$ kJ mol^{-1}). When higher temperatures are applied (i.e., entropy control), BrAN ($\Delta S^{\ddagger} = -136$ J mol^{-1} K^{-1}) becomes more reactive than MBriB ($\Delta S^{\ddagger} = -151$ J mol^{-1} K^{-1}). According to eq 5, one calculates for this pair an isokinetic temperature $T_{isokin} = -39.8$ °C, which is the temperature ($1/T = 0.0043$ K^{-1}) on the abscissa of Figure 3 where the two lines for bromoacetonitrile (BrAN) and methyl 2-bromoisobutyrate (MBriB) intersect.

$$T_{isokin} = \frac{\Delta\Delta H}{\Delta\Delta S} \qquad (5)$$

Further analysis of T_{isokin} is interesting for the couple MBrP/PEBr, which serves as model compounds for methyl acrylate and styrene polymerization, respectively. At temperatures higher than $T_{isokin} = 127$ °C activation of PEBr by Cu(I)Br-(PMDETA) is faster than of MBrP; at lower temperatures this reactivity order is reversed. Isokinetic temperatures for AllBr/ClAN and PEBr/ClPN pairs are 80 and 94 °C, respectively.

Conclusions

Activation rate constants for reactions of various alkyl halides as ATRP initiators with Cu(I)Br(PMDETA) were determined at various temperatures, and activation parameters were derived from the corresponding Eyring and Arrhenius plots. The activity of alkyl group for initiators generally follows the order tertiary > secondary > primary and nitrile > ester > benzyl. In accordance with transition state theory,[49] one finds that reactions of less active initiators are more accelerated by increased temperature than the corresponding reactions of more active alkyl halides. All obtained activation entropies ($\Delta S^{\ddagger}$) are highly negative, indicating that degrees of freedom are lost when approaching the transition state. Reactions of sterically less constrained initiators like nitriles and allyl bromide (AllBr) have the largest (least negative) activation entropies, which correspond to less rigid structures of the activated complexes. However, for the couples 2-bromopropionitrile (BrPN)/bromoacetonitrile (BrAN), 2-chloropropionitrile (ClPN)/chloroacetonitrile (ClAN), and methyl 2-bromoisobutyrate (MBriB)/methyl 2-bromopropionate (MBrP), it was found that an additional methyl group at the reaction center decreases the activation entropy by approximately 4−5 J mol^{-1} K^{-1}. This is probably caused by shorter copper−initiator distances for less active alkyl halides. In order to obtain an even more precise picture of the ATRP mechanism, the effect of temperature on the ATRP equilibrium constant (K_{ATRP})[50] is currently under investigation.

Acknowledgment. Financial support from the NSF (CHE-07-15494) and the CRP Consortium at CMU is gratefully acknowledged. F.S. gratefully acknowledges financial support from the German Academic Exchange Service (DAAD). We thank Michelle Coote and Patricia Golas for assistance during preparation of this manuscript.

Supporting Information Available: Details of the kinetic experiments; Eyring and Arrhenius plots. This material is available free of charge via the Internet at http://pubs.acs.org.

References and Notes

(1) Coessens, V.; Pintauer, T.; Matyjaszewski, K. *Prog. Polym. Sci.* **2001**, *26*, 337–377.
(2) Davis, K. A.; Matyjaszewski, K. *Adv. Polym. Sci.* **2002**, *159*, 1–166.
(3) Matyjaszewski, K. *Polym. Int.* **2003**, *52*, 1559–1565.
(4) Tsarevsky, N. V.; Matyjaszewski, K. *Chem. Rev.* **2007**, *107*, 2270–2299.
(5) Oh, J. K.; Drumright, R.; Siegwart, D. J.; Matyjaszewski, K. *Prog. Polym. Sci.* **2008**, *33*, 448–477.
(6) Sheiko, S. S.; Sumerlin, B. S.; Matyjaszewski, K. *Prog. Polym. Sci.* **2008**, *33*, 759–785.
(7) Gao, H.; Matyjaszewski, K. *Prog. Polym. Sci.* **2009**, *34*, 317–350.
(8) (a) Matyjaszewski, K. *J. Macromol. Sci., Pure Appl. Chem.* **1997**, *A34*, 1785–1801. (b) Coca, S.; Paik, H.-j.; Matyjaszewski, K. *Macromolecules* **1997**, *30*, 6513–6516. (c) Coca, S.; Matyjaszewski, K. *Macromolecules* **1997**, *30*, 2808–2810. (d) Matyjaszewski, K.; Gaynor, S. G. *Macromolecules* **1997**, *30*, 7042–7049. (e) Gaynor, S. G.; Matyjaszewski, K. *Macromolecules* **1997**, *30*, 4241–4243. (f) Shinoda, H.; Miller, P. J.; Matyjaszewski, K. *Macromolecules* **2001**, *34*, 3186–3194. (g) Shinoda, H.; Matyjaszewski, K. *Macromolecules* **2001**, *34*, 6243–6248. (h) Matyjaszewski, K.; Xia, J. *Chem. Rev.* **2001**, *101*, 2921–2990. (i) Braunecker, W. A.; Matyjaszewski, K. *Progr. Polym. Sci.* **2007**, *32*, 93–146.
(9) Goto, A.; Fukuda, T. *Prog. Polym. Sci.* **2004**, *29*, 329–385.
(10) Matyjaszewski, K. *J. Phys. Org. Chem.* **1995**, *8*, 197–207.
(11) Matyjaszewski, K.; Gaynor, S.; Greszta, D.; Mardare, D.; Shigemoto, T. *J. Phys. Org. Chem.* **1995**, *8*, 306–315.
(12) Braunecker, W. A.; Brown, W. C.; Morelli, B. C.; Tang, W.; Poli, R.; Matyjaszewski, K. *Macromolecules* **2007**, *40*, 8576–8585.
(13) Tang, W.; Matyjaszewski, K. *Macromolecules* **2006**, *39*, 4953–4959.
(14) Fischer, H. *J. Am. Chem. Soc.* **1987**, *108*, 3925–3927.
(15) Fischer, H. *Chem. Rev.* **2001**, *101*, 3581–3610.
(16) Tang, W.; Tsarevsky, N. V.; Matyjaszewski, K. *J. Am. Chem. Soc.* **2006**, *128*, 1598–1604.
(17) Wang, J.-S.; Matyjaszewski, K. *Macromolecules* **1995**, *28*, 7901–7910.
(18) Patten, T. E.; Xia, J.; Abernathy, T.; Matyjaszewski, K. *Science* **1996**, *272*, 866–868.
(19) Matyjaszewski, K.; Patten, T. E.; Xia, J. *J. Am. Chem. Soc.* **1997**, *119*, 674–680.
(20) Ohno, K.; Goto, A.; Fukuda, T.; Xia, J.; Matyjaszewski, K. *Macromolecules* **1998**, *31*, 2699–2701.
(21) Goto, A.; Fukuda, T. *Macromol. Rapid Commun.* **1999**, *20*, 633–636.
(22) Pascual, S.; Coutin, B.; Tardi, M.; Polton, A.; Vairon, J. P. *Macromolecules* **1999**, *32*, 1432–1437.
(23) Chambard, G.; Klumperman, B.; German, A. L. *Macromolecules* **2000**, *33*, 4417–4421.
(24) Matyjaszewski, K.; Goebelt, B.; Paik, H.-j.; Horwitz, C. P. *Macromolecules* **2001**, *34*, 430–440.
(25) Matyjaszewski, K.; Paik, H.-j.; Shipp, D. A.; Isobe, Y.; Okamoto, Y. *Macromolecules* **2001**, *34*, 3127–3129.

(26) Matyjaszewski, K.; Paik, H.-j.; Zhou, P.; Diamanti, S. J. *Macromolecules* **2001**, *34*, 5125–5131.
(27) Schellekens, M. A. J.; de Wit, F.; Klumperman, B. *Macromolecules* **2001**, *34*, 7961–7966.
(28) Matyjaszewski, K. *Macromolecules* **2002**, *35*, 6773–6781.
(29) (a) Pintauer, T.; Zhou, P.; Matyjaszewski, K. *J. Am. Chem. Soc.* **2002**, *124*, 8196–8197. (b) Pintauer, T.; Matyjaszewski, K. *Coord. Chem. Rev.* **2005**, *249*, 1155–1184.
(30) Nanda, A. K.; Matyjaszewski, K. *Macromolecules* **2003**, *36*, 599–604.
(31) Nanda, A. K.; Matyjaszewski, K. *Macromolecules* **2003**, *36*, 1487–1493.
(32) Nanda, A. K.; Matyjaszewski, K. *Macromolecules* **2003**, *36*, 8222–8224.
(33) Pintauer, T.; Braunecker, W.; Collange, E.; Poli, R.; Matyjaszewski, K. *Macromolecules* **2004**, *37*, 2679–2682.
(34) Matyjaszewski, K.; Nanda, A. K.; Tang, W. *Macromolecules* **2005**, *38*, 2015–2018.
(35) Tang, W.; Nanda, A. K.; Matyjaszewski, K. *Macromol. Chem. Phys.* **2005**, *206*, 1171–1177.
(36) Venkatesh, R.; Vergouwen, F.; Klumperman, B. *Macromol. Chem. Phys.* **2005**, *206*, 547–552.
(37) Tang, W.; Matyjaszewski, K. *Macromolecules* **2007**, *40*, 1858–1863.
(38) Bertin, D.; Gigmes, D.; Marque, S. R. A. *Recent Res. Dev. Org. Chem.* **2006**, *10*, 63–121.
(39) Beckwith, A. L. J.; Bowry, V. W.; Ingold, K. U. *J. Am. Chem. Soc.* **1992**, *114*, 4983–4992.
(40) Connors, K. A. *Chemical Kinetics*; VCH Publishers: New York, 1990.
(41) Blandamer, M. J.; Burgess, J.; Engberts, J. B. F. N. *Chem. Soc. Rev.* **1985**, *14*, 237–264.
(42) Lin, C. Y.; Coote, M. L.; Gennaro, A.; Matyjaszewski, K. *J. Am. Chem. Soc.* **2008**, *130*, 12762–12774.
(43) Zipse, H. *Top. Curr. Chem.* **2006**, *263*, 163–189.
(44) Gillies, M. B.; Matyjaszewski, K.; Norrby, P.-O.; Pintauer, T.; Poli, R.; Richard, P. *Macromolecules* **2003**, *36*, 8551–8559.
(45) Anslyn, E. V.; Dougherty, D. A. *Modern Physical Organic Chemistry*; University Science Books: Sausalito, CA, 2006.
(46) Hammond, G. S. *J. Am. Chem. Soc.* **1955**, *77*, 334–338.
(47) Miller, A. R. *J. Am. Chem. Soc.* **1978**, *100*, 1984–1992.
(48) Evans, M. G.; Polanyi, M. *Trans. Faraday Soc.* **1938**, *34*, 11–24.
(49) Albery, W. J. *Adv. Phys. Org. Chem.* **1993**, *28*, 139–170.
(50) Tang, W.; Kwak, Y.; Braunecker, W.; Tsarevsky, N. V.; Coote, M. L.; Matyjaszewski, K. *J. Am. Chem. Soc.* **2008**, *130*, 10702–10713.